Published in final edited form as:
Mol Pharmacol. 2008 October ; 74(4): 1141–1151. doi:10.1124/mol.108.049064.

Selective Inhibition of MAPK Phosphatases by Zinc Accounts for ERK1/2-dependent Oxidative Neuronal Cell Death

Yeung Ho*, **Ranmal Samarasinghe***, **Megan E. Knoch**, **Marcia Lewis**, **Elias Aizenman**, and **Donald B. DeFranco**

Department of Neuroscience, University of Pittsburgh, Pittsburgh, PA, 15260, USA (Y. H., R. S.); Department of Neurobiology, University of Pittsburgh School of Medicine, Pittsburgh, PA 15261, USA (M.K., E. A.); Department of Pharmacology and Pittsburgh Institute for Neurodegenerative Diseases, University of Pittsburgh School of Medicine, Pittsburgh, PA 15261, USA (D. B. D., M.L.)

Abstract

Oxidative stress induced by glutathione depletion in the mouse HT22 neuroblastoma cell line and embryonic rat immature cortical neurons causes a delayed, sustained activation of extracellular signal-regulated kinases-1/2 (ERK1/2), which is required for cell death. This sustained activation of ERK1/2 is mediated primarily by a selective inhibition of distinct ERK1/2-directed phosphatases either by enhanced degradation (i.e. for Mitogen activated protein kinase [MAPK] Phosphatase-1) or as shown here by reductions in enzymatic activity (i.e. for Protein Phosphatase type 2A [PP-2A]). The inhibition of ERK1/2 phosphatases in HT22 cells and immature neurons subjected to glutathione depletion results from oxidative stress as phosphatase activity is restored in cells treated with the antioxidant butylated hydroxyanisole (BHA). This leads to reduced ERK1/2 activation and neuroprotection. Furthermore, an increase in free intracellular zinc that accompanies glutathione-induced oxidative stress in HT22 cells and immature neurons contributes to selective inhibition of ERK1/2 phosphatase activity and cell death. Finally, ERK1/2 also functions to maintain elevated levels of zinc. Thus the elevation of intracellular zinc within neurons subjected to oxidative stress can trigger a robust positive feedback loop operating through activated ERK1/2 that rapidly sets into motion a zinc-dependent pathway of cell death.

Oxidative stress results from the accumulation of reactive oxygen species (ROS) and is brought about by a disruption of the physiological balance between normal oxidant production and various anti-oxidant defense systems. The brain is particularly sensitive to ROS accumulation and oxidative stress is implicated in the pathogenesis of many chronic neurodegenerative diseases as well as acute neuronal injury such as stroke (McCulloch and Dewar, 2001). Importantly, oxidative stress alters many metabolic and signaling pathways through effects on protein redox state and indirectly through triggering the release of intracellular stores of metal ions such as Zn^{2+}(Sensi and Jeng 2004). Zn^{2+} has been found to be toxic to neurons *in vitro* (Koh and Choi 1994) and intracellular Zn^{2+} accumulation plays a crucial role in ischemic injury (Koh et al., 1996) as well as other forms of neuronal cell death (Land and Aizenman 2005).

A number of cellular signaling pathways are activated by oxidative stress in neurons including the mitogen-activated protein kinases (MAPKs). MAPK members, including extracelluar-signal-regulated kinase (ERK1/2), Jun N-terminal kinase/stress-activated protein kinase (JNK/

Corresponding Author: Donald B. DeFranco, Department of Pharmacology, University of Pittsburgh School of Medicine, 7041 BST 3, 3501 Fifth Avenue, Pittsburgh, PA 15261, USA. Tel: +1-412-624-4259; Fax: +1-412-648-1945; E-mail: dod1@pitt.edu.
*Both authors contributed equally to this work and should be considered as first authors
Send reprint requests to: Donald B. DeFranco, Department of Pharmacology, 7041 Biomedical Sciences Tower 3, 3501 Fifth Avenue, University of Pittsburgh School of Medicine, Pittsburgh, PA 15260, dod1@pitt.edu

SAPK) and p38 MAPK kinase families, impact a variety of neuronal cell functions (Thomas and Huganir, 2004). The JNK/SAPK and p38 pathways are most often associated with neuronal cell death while ERK1/2 contributes to neuroprotection and survival (Xia et al., 1995). However, ERK1/2 has also been found to promote neuronal cell death in a number of *in vitro* models of neurodegeneration induced by oxidative stress (Levinthal and DeFranco, 2004; Satoh et al., 2000) or Zn^{+2} (Seo et al., 2001). In fact, pharmacological inhibition of ERK1/2 activation *in vivo* reduces neuronal cell injury in response to transient focal ischemia (Alessandrini et al., 1999).

Glutamate-induced oxidative toxicity in the HT22 neuroblastoma cell line (Li et al., 1997b) and primary immature cortical neurons (Murphy et al., 1990) has provided a useful model for studying the effects of oxidative stress on neuronal cell death. Both HT22 cells and immature neurons lack N-methyl-D-aspartate receptors but are depleted of glutathione upon glutamate-mediated inhibition of a glutamate/cystine antiporter (Murphy et al., 1990). Oxidative stress in HT22 cells and immature neurons triggers a form of cell death that has features of both apoptosis and necrosis (Li et al., 1997; Tan et al., 2001).

We have previously reported that oxidative stress in HT22 cells and immature neurons causes a biphasic activation of ERK1/2 with the delayed, sustained activation of ERK1/2 contributing to neuronal cell death (Luo and DeFranco, 2006; Stanciu and DeFranco, 2002). This sustained activation of ERK1/2 is mediated primarily by a selective, reversible inhibition of ERK1/2-directed phosphatases (Levinthal and DeFranco, 2005). In this study, we show that increased intracellular accumulation of Zn^{+2} in oxidatively stressed neuronal cells is responsible for the selective inhibition of ERK-phosphatases and ensuing ERK1/2 activation and cell death. Surprisingly, ERK1/2 also functions to maintain elevated levels of Zn^{+2}. Thus the elevation of intracellular Zn^{+2} within damaged neurons can trigger a robust positive feedback loop operating through activated ERK1/2 that rapidly sets into motion a Zn^{2+} -dependent pathway of cell death.

MATERIALS AND METHODS

Primary Neuron Cultures and Cell Lines

Primary neuron cultures were prepared from the cortices of embryonic 17 Sprague-Dawley rat fetuses (Hilltop Lab Animals, Scottsdale PA). Briefly, the cortices of embryonic 17 Sprague-Dawley rat fetuses were dissected and dissociated by repeated triturating in Hanks' balanced salt solution (5.4 mM KCl, 0.3 mM Na_2HPO_4, 0.4 mM KH_2PO_4, 4.2 mM $NaHCO_3$, 137 mM NaCl, 5.6 mM D-glucose, pH 7.4) without Ca^{2+} or Mg^{2+} (Invitrogen, Carlsbad CA). The cell suspensions were then passed through a 40-μm cell strainer (BD Biosciences, San Hosea CA) to remove clumped cells. Cells were then counted and plated on 50μg/ml poly-d-lysine coated cultures plates at a density of ~$1x10^5$ cells/cm^2. Cell viability was assessed by the uptake of trypan blue dye and was usually greater than 80%. Cultures were maintained for 2–3 days in media (Dulbecco's modified essential medium [DMEM], 10% fetal calf serum (Hyclone, Logan UT), 10% Ham's F12 nutrient supplement (Sigma, St. Louis MO), 1.9 mM glutamine, 24 mM Hepes buffer and 4.5 mg/ml glucose) at 37ºC and 5% CO_2. At this time, the mixed cortical cultures are ~80% neuronal, with ~20% glial fibrillary-associated protein staining cells (Murphy et al., 1990). HT22 cells were maintained in DMEM supplemented with 10% fetal bovine serum, 100 units of penicillin, and 100μg/ml streptomycin at 37ºC and 5% CO_2.

Cell Viability Assay

A DNA dye propidium iodide (PI) was used to assess cell viability. PI is excluded from healthy, intact cells and could only get access into cells with a compromised plasma membrane. 14–16 h after being treated with homocysteate (HCA), primary neurons were incubated for 10 min

in media containing a final concentration of 6.25 μg/ml PI. Cells were observed under an inverted fluorescence microscope equipped with phase-contrast optics (Nikon Eclipse TE200, Melville NY). Multiple fields were counted for each condition in at least 3 independent cultures with the total cells population of at least 500 neurons each condition. Toxicity was assessed in 5mM glutamate-treated HT22 cells at 12 h using the PI staining method described above.

ERK2- and JNK3-directed Phosphatase Activity Assay

A nonradioactive method has been modified for determining ERK2- and JNK3-directed phosphatase activity in cell lysates and is based on detecting dephosphorylation of a purified, dual-phosphorylated, His_6-tagged ERK2 or JNK3 upon incubation with the cell lysates (Levinthal and DeFranco, 2005). The alterations of ERK2 or JNK3 phosphatase activity within the cell lysates can be monitored by measuring changes in the phosphorylation state of the isolated phosphorylated ERK2 or JNK3 substrate, as shown by Western blotting with a phospho-specific ERK1/2 or JNK antibody. Briefly, 150 μg of cell lysates were diluted into a total volume of 250 μl in phosphatase assay buffer (10 mM $MgCl_2$, 10 mM Hepes, pH7.5 and 10 μM of the MEK inhibitor, U0126). Recombinant dual phosphorylated His_6-ERK2 or His_6-JNK3 (Biomol, Plymouth Meeting, PA) was added to each sample (30 ng/sample), and the reactions were maintained at 37ºC for 15 min where indicated. For the *in vitro* Zn^{2+} inhibition experiment, different concentrations of $ZnCl_2$ were pre-incubated with cell lysates for 10 min at 37ºC before the addition of purified pERK2 substrate. Following a 15 min incubation at 37ºC, reactions were stopped by the addition of 250 μl of wash buffer (8M urea, pH 8.6, containing 10 mM imidazole). 30μl of Ni^{2+}-conjugated, magnetic beads (Qiagen, Valencia CA) was then added to each reaction. After 90 min of rocking at 4ºC, the samples were washed twice with wash buffer followed by one wash in 300 mM NaCl, 25 mM Tris, pH 7.5. The beads were then suspended in Laemmli sample buffer, boiled for 5 min, loaded onto a 10% polyacrylamide gel, transferred to a polyvinylidine fluoride membrane (Millipore, Bedford MA) and subjected to Western blotting to detect phosphorylated ERK1/2, total ERK1/2, phosphorylated JNK3 or total JNK3.

PP2A Phosphatase Assay

The immunoprecipitation (IP) assay for PP2A activity was performed using procedures outlined in a PP2A IP assay kit (Millipore, Bedford MA). Briefly, PP2A was immunoprecipitated from HT22 cell lysates prepared in a PP2A phosphatase assay lysis buffer using a monoclonal antibody against the C subunit of PP2A. A sample of the immunoprecipitate was analyzed for recovery of PP2A C subunit by Western blotting. PP2A activity in the remainder of the immunoprecipitates was measured using a synthetic phosphopeptide substrate and a malachite green detection system for released phosphate (Millipore, Bedford MA). Activity measurements expressed as pmoles phosphate released were normalized to total PP2A C subunit recovered within individual immunoprecipitates.

Western Blot Analysis

Cells were treated with HCA or glutamate, scraped and collected in 1x PBS and then centrifuged at 7000 rpm for 3 min. The pellets were then disrupted in lysis buffer (50 mM Tris-Cl, pH 7.5, 2 mM EDTA, 100 mM NaCl, 1% Nonidet P-40, supplemented with protease inhibitor (Protease inhibitor cocktail, Sigma, St. Louis MO). The solubilized lysates were then centrifuged at 13,000 rpm for 5 min at 4ºC and supernatants were collected for further analysis. Protein concentrations of the extracts were determined using the Bio-rad reagent. Equivalent amount of total protein (20–30 μg) were separated by SDS-PAGE on 10% polyacrylamide gels and then transferred to polyvinylidine membranes. Membranes were blocked with 5% dry milk in PBS/0.1% (v/v) Tween 20 (PBST) for 1 h at room temperature. Membranes were then incubated with primary antibodies (anti-phospho-ERK1/2, anti-total ERK1/2, anti-phospho-

JNK, anti-total JNK, all from Cell Signaling (Danvers MA) overnight at 4ºC with 2% BSA in PBST. The membranes were then washed three times with PBST (10 min each time), incubated with the appropriate horseradish, peroxidase-conjugated secondary antibody for 40 min at room temperature and followed by three time washes with PBST. Immunoreactive bands were then revealed by enhanced chemiluminescence (ECL, GE Lifesciences, Piscataway NJ) using standard x-ray film (Eastman Kodak Co, Rochester NY). Densitometry was performed using a Personal Densitometer SI (GE Lifesciences, Piscataway NJ) linked to the ImageQuant 5.2 software (GE Lifesciences, Piscataway NJ).

Intracellular Zinc Imaging

Neuronal cultures were incubated in a Fluozin-3 AM (5 μM, Invitrogen, Carlsbad CA)-containing solution composed of HEPES-buffered saline, supplemented with 5 mg/mL BSA, for approximately 30 min. Immediately following incubation, coverslips were submerged in a recording chamber (Warner Instruments, Hamden CT) mounted on an inverted epifluorescence microscope (Nikon Eclipse TE200, Melville NY) equipped with a 10X and a 20X objective. MEM-HEPES-BSA was continuously perfused through the recording chamber via a gravity-driven perfusion system. Using a computer-controlled monochromator (Polychrome II, TILL Photonics, Germany) and a CCD camera (IMAGO, TILL Photonics, Germany), images were acquired with 490 nm excitation light. Once a series of baseline fluorescence images were established, a 20 μM Tetrakis-(2-pyridylmethyl)ethylenediamine (TPEN) solution was perfused through the chamber to chelate intracellular zinc and quench the fluorescent signal. The relative fluorescence for all cells (n= 6–40) was determined by subtracting the TPEN-quenched signal from the initial fluorescence and an average value was calculated for each coverslip (n=6). Data were analyzed and plotted using Origin 6.0 (OriginLab Corporation, Northampton MA).

Transfection and Luciferase Assay

Transfection of HT22 cells was performed with LipofectAMINE 2000 as described earlier (Hara and Aizenman, 2004). Cells were cotransfected with a HT22 cells were transfected with a firefly luciferase-containing plasmid driven by four tandem metal regulatory element (MRE) sequences (Hara and Aizenman, 2005) and a constitutively expressed *Renilla* luciferase plasmid (pRLTK), which serves as an internal control. Twenty-four hours after transfection, cells were stimulated with 5 mM glutamate alone or in the presence of 1 μM TPEN for 6 hours. Cells were then incubated overnight with the non-selective cysteine protease inhibitor bocaspartyl (OMe)-fluoromethylketone (BAF, 20 μM) to minimize oxidative damage to the cells and maximize MRE-driven expression. Firefly and *Renilla* luciferase activity were then measured using the Dual-Glo assay system (Promega).

Statistics

Comparison of two means was performed using a paired *t* test. Comparison of multiple mean values were performed by analysis of variance with either Turkey's or Bonferroni's *post hoc* tests for significance. p value of <0.05 were considered to be significant. All data were analyzed using GraphPad Prism version 4.0 for Windows (GraphPad Software, San Diego CA).

RESULTS

ERK2-directed phosphatase activity is inhibited during oxidative toxicity in HT22 cells and immature neurons

We had previously reported that glutamate-induced oxidative stress in immature neurons inhibits ERK2-directed phosphatases resulting in sustained activation of ERK1/2 (Levinthal and DeFranco, 2005). As HT22 cells exhibit analogous ERK1/2-dependent oxidative toxicity,

we first set out to examine if ERK1/2-directed phosphatases were inhibited by glutamate treatment in HT22 cells analogous to previously published results in immature neurons (Levinthal and DeFranco, 2005). An *in vitro* phosphatase assay was therefore used with whole cell lysates to dephosphorylate purified, dual-phosphorylated, His_6-tagged ERK2 (Levinthal and DeFranco, 2005). A nonspecific dual specificity phosphatase, lambda protein phosphatase, was employed as a positive control for ERK2 dephosphorylation (Fig. 1A).

As shown in Figure 1A, whole cell lysates prepared from HT22 cells possess robust ERK2 phosphatase activity, which was decreased upon a 7.5 h glutamate treatment of the cells (Fig. 1A). All phosphatase assays reported in this manuscript were performed after lengths of glutamate (or HCA) treatment that did not lead to overt signs of cell death (e.g. rounding and loss of adherence) but sufficient to generate oxidative stress (Levinthal and DeFranco, 2005). Quantification of four independent experiments revealed a significant increase ($p<0.05$) in the normalized levels of phosphorylated ERK2 in HT22 cell lysates exposed to glutamate for 7.5 h when compared to untreated cultures (Fig. 1B). When cells were exposed to shorter treatments with glutamate (i.e. 2 h and 5 h), ERK2 phosphatase activity was not significantly affected (Fig. 1A). The length of glutamate exposure that leads to inhibition of ERK2 phosphatase activity in HT22 cells is coincident with that required for maximal oxidative and enhanced ERK1/2 phosphorylation (Stanciu et al., 2002).

To confirm the effect of glutamate on the inhibition of ERK2 phosphatase activity in immature neurons, we used the glutamate analog homocysteate (HCA) to induce oxidative stress. HCA is a glutamate analog that has a relatively high binding affinity to glutamate/cysteine antiporter. While glutamate has been widely used to induce oxidative toxicity to immature neurons, we and others (Ryu et al., 2003) have found that HCA generates more reliable and reproducible toxicity and less variation between neuronal cultures. The ERK2 phosphatase assay was performed with whole cell lysates prepared from cultures treated with HCA for different times (i.e, 12 h, 14 h and 16 h). As shown in Figure 1C, a 14h or 16h treatment of neurons with HCA led to the inhibition of ERK2 phosphatase activity (Figs. 1C,1D).

Phosphorylated ERK1/2 is a substrate for various phosphatases including members of the protein serine/threonine phosphatase (PSTP) and dual specificity protein phosphatase (DSP) families (Farooq and Zhou, 2004). In fact, glutamate treatment of HT22 cells and immature neurons was recently shown to trigger the degradation of the DSP, MKP1 (Choi et al., 2006), which we confirmed in our cells (data not shown). However, since the inhibition of ERK1/2 phosphatase activity in glutamate–treated immature neurons is reversible (Levinthal and DeFranco, 2005), global degradation of ERK1/2 phosphatases is not solely responsible for persistent ERK1/2 activation. We therefore used IP to selectively analyze the effects of glutamate on the activity of PP2A, a PSTP that is one of the predominant ERK1/2 phosphatases expressed in neurons (Levinthal and DeFranco, 2005). As shown in Figure 1E, glutamate treatment of HT22 cells led to a significant decrease in PP2A activity, when normalized for total PP2A catalytic subunit recovered in immunoprecipitates. The levels of PP2A catalytic subunit in HT22 cells were not reduced upon glutamate treatment (Fig. 1E). Therefore, oxidative stress in neurons may limit ERK1/2 phosphatase activity by effecting either select phosphatase expression (e.g. MKP1) (Choi et al., 2006) or activity (e.g. PP2A).

An antioxidant that blocks oxidative toxicity reduces ERK1/2 activation and restores ERK2 phosphatase activity

The antioxidant, butylated hydroxyanisole (BHA) protects against glutamate-induced oxidative toxicity in immature neurons (Ryu et al., 2003) and HT22 cells (data not shown). BHA also prevents the oxidative stress-induced inhibition of JNK phosphatases and tumor necrosis factor-alpha (TNF-α) induced cell death in fibroblast cell lines (Kamata et al., 2005). The effects of BHA in blocking ERK1/2 activation induced by oxidative stress has also been

observed in other cell types such as head and neck squamous carcinoma cell (Kim et al., 2006a). We therefore used BHA to assess whether ERK1/2 activation and the inhibition of ERK2-directed phosphatase activity is mediated by ROS.

As shown in Figure 2A, a 7.5 h glutamate treatment induced significant ERK1/2 activation in HT22 cells. In immature neurons, HCA activation of ERK1/2 was evident at 14 h and peaked at 16 h (Fig. 2B), analogous to the time course of ERK1/2 activation by glutamate in immature neurons (Levinthal and DeFranco, 2005; Stanciu et al., 2002). The administration of BHA blocked ERK1/2 activation induced by oxidative stress in HT22 cells and neurons (Figs. 2A, 2B).

To investigate the mechanism responsible for BHA inhibition of ERK1/2 activation, ERK2 phosphatase assays were performed using cell lysates prepared from oxidatively stressed HT22 cells and neurons. As shown in Figures 2C and 2E, BHA prevented the inhibition of ERK2 phosphatase activity following glutamate treatment in HT22 cells. Similarly, BHA abrogated the inhibition of ERK phosphatase activity in neurons subject to HCA treatment (Figs. 2D & 2F). Thus, ROS-mediated inhibition of protein phosphatase activity is responsible, in part for the activation of ERK1/2 in oxidatively stressed neurons.

Selective inhibition of ERK2 phosphatase activity by Zn^{2+} in neuronal cell extracts

ERK1/2 phosphatases such as MKPs and PP2A are reversibly inactivated by thiol oxidation (Foley et al., 2004). Previously, we found that ERK2 phosphatase activity in extracts prepared from oxidatively stressed neurons was restored by the *in vitro* addition of DTT (Levinthal and DeFranco, 2005). Thus, oxidative inhibition of ERK1/2 phosphatases in HT22 cells and primary cortical neurons may occur through direct or indirect thiol oxidation of the phosphatases. However, DTT in addition to its well-known thiol reducing properties is also an effective Zn^{2+} chelating agent (Cornell and Crivaro, 1972). Thus, restoration of ERK2 phosphatase activity in extracts prepared from oxidatively stressed neurons by DTT may not be solely due to reduction of oxidized thiols. Interestingly, Zn^{2+} inhibits purified phosphatases that could act on ERK1/2 including the PSTP, PP2A (Zhuo and Dixon, 1997) and protein tyrosine phosphatases (PTPs) (Maret et al., 1999). As such, we investigated the effect of Zn^{2+} on ERK2 phosphatase activity.

As shown in Figure 3A, a 10 min preincubation of HT22 cell lysates with $ZnCl_2$ caused a concentration-dependent inhibition of ERK2 phosphatase activity with the maximal inhibition observed at 10μM. It must be noted, however, that the actual concentration of "free" Zn^{2+} is likely to be much lower that what we have added due to the various constituents of the cell extract and assay buffer that would bind to this metal. Therefore, it is entirely possible that the actual inhibitory concentrations of Zn^{2+} are very low, even in the nM range (Frederickson et al., 2006). Quantification of several independent experiments revealed a significant inhibition of ERK2 phosphatase activity by added zinc at 10μM (Figure 3B, $p<0.01$). ERK2 phosphatase activity measured in HT22 cell extracts is not sensitive to Fe^{+2} (Fig. 3C), another metal associated with oxidative toxicity in HT22 cells and immature cortical neurons (Zaman et al., 1999). This result is consistent with studies establishing stimulatory effects of Fe^{+2} on PP2A (Yu, 1998), the major ERK2 phosphatase reversibly affected by glutamate in HT22 cells (Fig. 1E).

To determine if the Zn^{2+} inhibition of phosphatase activity is specific to ERK phosphatases, we then examined Zn^{2+} effects on JNK3 phosphatase activity. As shown in Figure 3D, $ZnCl_2$ did not affect JNK3 phosphatase activity in HT22 cell lysates suggesting that exogenous Zn^{2+} is selective in inhibiting ERK2-directed phosphatases in HT22 cell extracts. This is not surprising since oxidative toxicity in HT22 cells and immature neurons is not associated with an increase in JNK activation or an inhibition of JNK phosphatase activity (Levinthal and

DeFranco, 2005). Furthermore, active p38 MAPK is not detected in unstimulated or glutamate treated HT22 cells (Levinthal and DeFranco, 2005).

HT22 cells were also treated with $ZnCl_2$ in order to establish whether Zn^{2+} can be directly responsible for ERK1/2 activation *in vitro* irrespective of oxidative stress. As shown in Figure 4A treatment of HT22 cells with 10 μM $ZnCl_2$ in the presence of the Zn^{2+} carrier sodium pyrithione (i.e. at 5 μM) led to a rapid and robust increase in ERK1/2 phosphorylation. This rapid ERK1/2 activation is not due to secondary generation of ROS, as it was not affected by the addition of the antioxidant BHA (Fig. 4B). Finally, rapid Zn^{2+}-dependent, ROS-independent ERK1/2 activation was associated with an inhibition of ERK2 phosphatase activity in HT22 cell lysates (Fig. 4C) confirming a direct role for Zn^{2+} in phosphatase inhibition.

Oxidative stress triggers Zn^{2+} accumulation in HT22 cells and primary neurons

The impact of oxidative stress in HT22 cells and immature neurons on intracellular Zn^{2+} accumulation was assessed using FluoZin 3-AM, a fluorescent Zn^{2+} indicator dye (Devinney et al., 2005). Relative intracellular Zn^{2+} levels was obtained by quantitative measures of FluoZin-3AM fluorescence within individual cells that is quenchable by the Zn^{2+} chelator, N,N,N′,N′-Tetrakis-(2-pyridylmethyl)-Ethylenediamine (TPEN; Knoch et al. 2008). As shown in Figure 5A, oxidative stress in HT22 cells and immature neurons led to a doubling of the relative TPEN-quenchable FluoZin 3-AM fluorescence. Thus oxidative stress in both HT22 cells and immature neurons trigger the accumulation of intracellular Zn^{2+}, similar to what we have reported in other systems (Aizenman et al., 2000; Zhang et al., 2004).

To confirm these findings, we used a molecular assay that measures specific Zn^{2+} driven gene expression. HT22 cells were transfected with a firefly luciferase-containing plasmid driven by four tandem MRE sequences (Hara and Aizenman, 2005). The MRE sequence is found in Zn^{2+} regulated genes, including metallothionein. MRE-driven gene expression is activated following the binding of Zn^{2+} to the MTF-1 transcription factor-1. As shown in Figure 5A (inset), MRE-driven luciferase expression was significantly increased in the glutamate-treated cells, while this effect was completely abrogated by TPEN. This result strongly indicates that during glutamate-induced oxidative stress, sufficient intracellular Zn^{2+} was liberated to trigger MTF-1/MRE-driven gene expression.

In order to determine the relationship between oxidant production, intracellular Zn^{2+} accumulation and ERK1/2 activation, neurons were exposed to HCA in the presence or absence of either the antioxidant BHA or the MEK1/2 inhibitor U0126. As shown in Figure 5B, BHA blocked HCA-induced intracellular Zn^{2+} accumulation and exerted no significant effect on the relative intracellular Zn^{2+} levels when given alone. Interestingly, U0126 treatment also reduced TPEN-quenchable Zn^{2+} fluorescence in HCA-treated neurons and did not alter Zn^{2+} levels when given alone (Fig. 5B). Thus Zn^{2+} accumulation triggered by ROS may be exacerbated through a positive feedback loop driven by activated ERK1/2.

Chelation of intracellular Zn^{2+} blocks ERK1/2 activation and restores ERK2 phosphatase activity

Zn^{2+}-induced ERK1/2 activation has been reported to contribute to neuronal cell death (Seo et al., 2001; Zhang et al., 2004). To evaluate the role of Zn^{2+} accumulation in activating ERK1/2 in HT22 cells and primary neurons, we employed the high affinity Zn^{2+} chelator TPEN. HT22 cells were treated with glutamate, in the presence or absence of 1 μM and 5 μM TPEN for 8 h. Whole cell lysates were then subject to Western blot analysis to detect phosphorylated, activated ERK1/2. As shown in Figure 6A, exposure of HT22 cells to glutamate induced a large increase in ERK1/2 phosphorylation that was unaffected by the addition of 1 μM TPEN.

However, the addition of 5 μM TPEN significantly blocked glutamate-induced ERK1/2 activation (Fig. 6A). This result suggests that ERK1/2 activation is downstream of Zn^{2+} accumulation.

Similar experiments were then extended to immature neurons, which were treated with HCA, HCA plus 1 μM TPEN and HCA plus 5 μM TPEN for 16 h. Analogous to results obtained in HT22 cells, addition of 5 μM but not 1 μM TPEN significantly blocked the activation of ERK1/2 following oxidative stress in primary neurons (Fig. 6B).

Given the fact that Zn^{2+}inhibits ERK2 phosphatase activity *in vitro* (Figs. 3A, 3B), we set out to examine whether TPEN inhibition of ERK1/2 activation occurs through the reversal of Zn^{2+}-mediated inhibition of ERK1/2 phosphatases. The ERK2 phosphatase assay was performed on whole cell lysates prepared from untreated HT22 cells, or cells treated with glutamate, glutamate plus 1 μM or 5 μM TPEN. As shown in Figures 6C and 6E, ERK2 phosphatase activity was decreased following treatment with glutamate. The addition of 1 μM TPEN to HT22 cells did not reverse this inhibitory effect of glutamate (Figs. 6C, 6E). However, the addition of 5 μM TPEN significantly reversed the inhibition of ERK2 phosphatase activity in HT22 cells that were treated with glutamate (Figs. 6C, 6E). Similar results were obtained in primary neurons (Figs. 6D, 6F). These results suggest that TPEN blocks Zn^{2+}-induced ERK1/2 activation by reversing a Zn^{2+}-mediated inhibition of ERK1/2 phosphatase activity.

As U0126 has been found to block Zn^{2+} accumulation in oxidatively-stressed cells (Fig. 5), we sought to examine whether U0126 could also reverse the inhibition of ERK2 phosphatase activity. The ERK2 phosphatase assay were therefore performed on cell lysates prepared from untreated HT22 cells or cells treated with glutamate or glutamate plus U0126. As shown in Figures 6G and 6H, U0126 treatment of HT22 cells reversed the inhibition of ERK2 phosphatase activity induced by oxidative stress. This result reinforces the notion that activated ERK1/2 contributes to a positive feedback loop that maintains elevated levels of intracellular $Zn^{2+}$and persistent inhibition of ERK1/2 phosphatases.

TPEN protects neuronal cells from oxidative toxicity

We then set out to examine whether TPEN could also limit cell death. Due to the fact that Zn^{2+} is an essential metal, we limited TPEN treatment to less than 16 h in both HT22 cells and primary neurons. Prolonged exposure (i.e. 48 h) of HT22 cells and primary neurons with TPEN alone is toxic (data not shown). HT22 cells were treated for 12 h with glutamate, glutamate plus 1 μM TPEN, glutamate plus 5 μM TPEN as well as 1 μM TPEN and 5 μM TPEN alone. A propidium iodide (PI) staining method was then used to assess cell toxicity (Levinthal and DeFranco, 2005). As shown in Figure 7A, a significant proportion of HT22 cells stained positive for PI upon glutamate treatment. Cells treated with glutamate plus 1 μM TPEN exhibited a similar extent of cell death. However, a 5 μM TPEN treatment significantly protected HT22 cells from glutamate-induced cell death (Fig. 7A, $p<0.001$). This neuroprotective effect is similar to that provided by U0126 (Fig. 7A). A 12 h treatment with 1 μM and 5 μM TPEN alone exhibited no toxicity in HT22 cells (Fig. 7A).

This paradigm was then extended to immature neurons. These cultures were subject to the same treatment as HT22 cells and cell toxicity assessed after treatment for 16 h. Similar to the results obtained in HT22 cells, a 16 h treatment with HCA as well as HCA plus 1 μM TPEN induced significant cell death in immature neurons (Fig. 7B). However, the addition of 5 μM TPEN significantly protected immature neurons from HCA-induced toxicity (Fig. 7B). In summary, the dose of TPEN required to protect both HT22 cells and immature neurons from oxidative toxicity is coincident with that required to block ERK1/2 activation and ERK1/2 phosphatase inhibition.

The contribution of Fe^{2+} to neuronal oxidative toxicity was previously revealed with experiments demonstrating neuroprotective effects of Fe^{2+} chelation (Zaman et al., 1999). Since TPEN can also chelate Fe^{2+}, the metal selectivity of its neuroprotective actions was tested by the co-application of TPEN with either Fe^{2+} or Zn^{2+}. As shown in Figure 7C, inclusion of Zn^{2+} completely blocked the neuroprotective effect of TPEN in glutamate treated HT22 cells ($p<0.001$). In contrast, addition of Fe^{2+} only partially reversed the actions of TPEN, suggesting that Zn^{2+} is a more important contributor to the oxidative toxicity observed in our system.

DISCUSSION

ERK1/2 functions in many cell types to promote proliferation or survival but can also be diverted to participate in certain cell death pathways. For example, chronic activation of ERK1/2 is necessary for cell death induced by oxidative stress in immature neurons and HT22 cells (Luo and DeFranco, 2006; Satoh et al., 2000). In these cases, the inhibition of select protein phosphatases is primarily responsible for the persistent activation of ERK1/2 (Levinthal and DeFranco, 2005). This conclusion was confirmed in a recent report, which also revealed the minimal contribution of upstream activating kinases (i.e. MEK1/2) to prolonged ERK1/2 activation in oxidatively stressed HT22 cells and immature neurons (Choi et al., 2006).

We show here that the inhibition of ERK1/2 phosphatases in HT22 cells and immature neurons subjected to glutathione depletion is indeed the result of oxidative stress as phosphatase activity is restored in cells treated with BHA. This leads to reduced ERK1/2 activation and neuroprotection. The oxidative inhibition of protein phosphatase activity in TNF-α treated fibroblasts is also eliminated by BHA treatment (Kamata et al., 2005). However in TNF-α induced oxidative toxicity and Concanavolin A-induced liver toxicity in mice, cell death is associated with the selective inhibition of JNK phosphatases (Kamata et al., 2005). Glutamate-induced oxidative stress in immature neurons does not significantly affect JNK phosphatase activity (Levinthal and DeFranco, 2005). Therefore, even though MAPK phosphatases are oxidant sensitive, they are not globally inactivated by oxidative stress in cells. Depending upon the nature of the oxidative stress imposed upon living cells, select MAPK phosphatases may be protected from the damaging effects of reactive species due to their sequestration within subcellular compartments or multi-subunit complexes that are inaccessible to short-lived oxidants.

While several protein phosphatases are redox sensitive and inhibited by direct thiol oxidation of a catalytic-site cysteine (Meng et al., 2002; Tonks, 2003), our results suggest that MAPK phosphatase activity may also be regulated in oxidatively stressed cells by the inhibitory effects of free Zn^{2+}. Zn^{2+} effects on ERK1/2 activation have been observed in neurons (Seo et al., 2001), but our results identify the molecular target of Zn^{2+} that is responsible for this effect. The sensitivity of various MAPK phosphatases to inhibition by Zn^{2+} was established with purified phosphatase preparations suggesting that Zn^{2+} can act directly to impact the activity of these enzymes (Zhuo and Dixon, 1997). Zn^{2+} mediated inhibition of PTPs has been suggested to impact insulin/insulin-like growth factor (Haase and Maret, 2003) or interleukin-8 (Kim et al., 2006b) signaling in C6 glioblastoma or BEAS-2B human airway epithelial cells, respectively. Thus, Zn^{2+}-mediated inhibition of protein phosphatase activity may not always be linked to cell death responses but could play a role in facilitating hormone signaling (Haase and Maret, 2003). However, prolonged inhibition of select MAPK phosphatases and ensuing persistent activation of specific MAPKs that drives toxicity in oxidatively stressed cells may reflect an inability to restore Zn^{2+} homeostasis (see below).

For PSTPs, Zn^{2+} may exert its inhibitory effects through the displacement of bound Mn^{+2} at the active site of their catalytic subunits (Zhuo and Dixon, 1997). Interestingly, purified PSTPs such as PP2A are refractory to exchange by Mn^{2+} once bound by Zn^{2+} and therefore limited

recovery of their activity can be achieved by Zn^{2+} chelation *in vitro* (Zhuo and Dixon, 1997). These potent inhibitory effects of Zn^{2+} on ERK1/2 phosphatases such as PP2A may explain the requirement for a 5 μM TPEN treatment to reverse the inhibition of ERK1/2 phosphatase activity in oxidatively stressed HT22 cells and immature neurons. Importantly, 5 μM TPEN was also required to block glutamate- and HCA-induced toxicity in HT22 cells and immature neurons, respectively, showing a close association between the inhibition of ERK1/2 activation, restoration of ERK1/2 phosphatase activity and protection from oxidative stress.

Since selective iron chelators block HCA-induced toxicity in immature neurons (Zaman et al., 1999) it is likely that TPEN exerts its protective effects via chelation of Fe^{2+} as well as Zn^{2+}. However, Fe^{2+} contributes indirectly to ERK1/2 phosphatase inhibition through its impact on ROS generation in HT22 cells and immature neurons unlike Zn^{2+}, which exerts a direct inhibitory effect on ERK1/2 phosphatases. Select phosphatase inhibition is also partially responsible for ERK1/2 activation in distinct brain regions vulnerable to a global ischemia insult (Ho et al., 2007). It remains to be established whether oxidative stress and/or intracellular free Zn^{2+} contributes to regional inhibition of ERK1/2 phosphatases in ischemic brain.

Previous results from our group suggest that PP2A is the major ERK1/2 phosphatase in immature neurons (Levinthal and DeFranco, 2005) and HT22 cells (data not shown) but other MAPK phosphatases in these cells contribute to the regulation of ERK1/2 activation. In a recent report, glutamate treatment of HT22 cells and immature neurons was found to trigger the degradation of MKP1 (Choi et al., 2006). While MKP1 exerts a minor albeit significant effect on ERK1/2 activation and glutamate toxicity in HT22 cells (Choi et al., 2006), the loss of this enzyme cannot be solely responsible for heightened ERK1/2 activation since ERK1/2 phosphatase activity in extracts from oxidatively stressed neurons can be restored *in vitro* with DTT (Levinthal and DeFranco, 2005). Furthermore, the JNK family of MAPKs is the preferred substrates of MKP1, which is inconsistent with the selective effects of oxidative stress in HT22 cells and immature neurons on ERK1/2 phosphatases. Since PP2A activity but not protein expression (i.e. of its C subunit) was reduced in glutamate-treated HT22 cells, oxidative stress in neurons can trigger both reversible (Levinthal and DeFranco, 2005) and irreversible (Choi et al., 2006) alterations in distinct protein phosphatases that collectively could contribute to persistent activation of specific MAPKs.

The decreased accumulation of free Zn^{2+} upon inhibition of ERK1/2 activation by U0126 supports the existence of a positive feedback loop that not only provides conditions for the maintenance of ERK1/2 activation (i.e. through phosphatase inhibition) but also exacerbates neuronal cell exposure to neurotoxic levels of free Zn^{2+} (Fig. 7). In this case, ROS, which contribute to ERK1/2 activation in an 12-lipoxygenase (12-LOX)-dependent manner ((Stanciu et al., 2000); Fig. 8), provide the trigger that acts to promote the release of protein-bound Zn^{2+}, perhaps through thiol oxidation of specific cysteine residues that participate in Zn^{2+} binding (Aizenman et al., 2000). Thus, ERK1/2 may prevent the repair of oxidatively damaged Zn^{2+} binding proteins or limit their expression (Jiang et al., 2004). In the absence of oxidative damage to these proteins, chronic ERK1/2 activation may not impact intracellular Zn^{2+} homeostasis and promote cell death.

In summary, we have identified an important regulatory feature of protein phosphatase regulation, namely, reversible Zn^{2+} inhibition that triggers the persistent activation of a select MAPK signaling module in neurons. Furthermore, the oxidative induction of Zn^{2+} accumulation predisposes neuronal cells to a positive feedback loop driven by ERK1/2 that disrupts Zn^{2+} homeostasis and further exacerbates cellular exposure to neurotoxic levels of free Zn^{2+}.

Acknowledgements

We thank David Schubert (Salk Institute) for the kind gift of HT22 cells and David Giedroc (University of Indiana) for the MRE-luciferase plasmid. We thank Dr Karl Kandler for invaluable help and advice on the quantitative fluorescence measurement and for the use of his equipment. We also thank Karen Hartnett for expert technical assistance.

This work was supported by NIH grant NS38319 (DBD) and NS43277 (EA)

Abbreviations

MAPK
mitogen-activated protein kinase

ERK
extracellular-signal-regulated kinase

PP-2A
protein phosphatase-type 2A

BHA
butylated hydroxyanisole

ROS
reactive oxygen species

JNK/SAPK
Jun N-terminal kinase/stress-activated protein kinase

MEK
MAPK kinases

MKKK
MEK/MKK kinases

DMEM
Dulbecco’s Modified Essential Medium

HCA
homocysteate

MRE
metal regulatory element

MTF-1
metal regulatory element transcription factor-1

BAF
bocaspartyl (OMe)-fluoromethylketone

PI
propidium iodine

PBST
phosphate buffered saline with Tween-20

IP
immunoprecipitation

DTT
dithiothreitol

PSTP
protein serine/threonine phosphatase

DSP
dual-specificity protein phosphatase

PTP
protein-tyrosine phosphatase

TPEN
N,N,N′,N′-Tetrakis-(2-pyridylmethyl)-Ethylenediamine

TNF-α
tumor necrosis factor-alpha

12-LOX
12-lipoxygenase

DTDP
2,2′-dithhildipyridine

References

Aizenman E, Stout AK, Hartnett KA, Dineley KE, McLaughlin B, Reynolds IJ. Induction of neuronal apoptosis by thiol oxidation: putative role of intracellular zinc release. JNeurochem 2000;75(5):1878–1888. [PubMed: 11032877]

Alessandrini A, Namura S, Moskowitz MA, Bonventre JV. MEK1 protein kinase inhibition protects against damage resulting from focal cerebral ischemia. Proc Natl Acad Sci USA 1999;96(22):12866–12869. [PubMed: 10536014]

Choi BH, Hur EM, Lee JH, Jun DJ, Kim KT. Protein kinase Cdelta-mediated proteasomal degradation of MAP kinase phosphatase-1 contributes to glutamate-induced neuronal cell death. J Cell Sci 2006;119(Pt 7):1329–1340. [PubMed: 16537649]

Cornell NW, Crivaro KE. Stability constant for the zinc-dithiothreitol complex. Anal Biochem 1972;47(1):203–208. [PubMed: 5031113]

Devinney MJ 2nd, Reynolds IJ, Dineley KE. Simultaneous detection of intracellular free calcium and zinc using fura-2FF and FluoZin-3. Cell Calcium 2005;37(3):225–232. [PubMed: 15670869]

Farooq A, Zhou MM. Structure and regulation of MAPK phosphatases. Cell Signal 2004;16(7):769–779. [PubMed: 15115656]

Foley TD, Armstrong JJ, Kupchak BR. Identification and H2O2 sensitivity of the major constitutive MAPK phosphatase from rat brain. Biochem Biophys Res Commun 2004;315(3):568–574. [PubMed: 14975738]

Frederickson CJ, Giblin LJ, Krezel A, McAdoo DJ, Mueller RN, Zeng Y, Balaji RV, Masalha R, Thompson RB, Fierke CA, Sarvey JM, de Valdenebro M, Prough DS, Zornow MH. Concentrations of extracellular free zinc (pZn)e in the central nervous system during simple anesthetization, ischemia and reperfusion. Exp Neurol 2006;198(2):285–293. [PubMed: 16443223]

Haase H, Maret W. Intracellular zinc fluctuations modulate protein tyrosine phosphatase activity in insulin/insulin-like growth factor-1 signaling. Exp Cell Res 2003;291(2):289– 298. [PubMed: 14644152]

Hara H, Aizenman E. A molecular technique for detecting the liberation of intracellular zinc in cultured neurons. J Neurosci Methods 2004;137(2):175–180. [PubMed: 15262058]

Ho Y, Logue E, Callaway CW, DeFranco DB. Different mechanisms account for extracellular-signal regulated kinase activation in distinct brain regions following global ischemia and reperfusion. Neuroscience 2007;145(1):248–255. [PubMed: 17207579]

Jiang H, Fu K, Andrews GK. Gene- and cell-type-specific effects of signal transduction cascades on metal-regulated gene transcription appear to be independent of changes in the phosphorylation of metal-response-element-binding transcription factor-1. Biochem J 2004;382(Pt 1):33–41. [PubMed: 15142038]

Kamata H, Honda S, Maeda S, Chang L, Hirata H, Karin M. Reactive oxygen species promote TNFalpha-induced death and sustained JNK activation by inhibiting MAP kinase phosphatases. Cell 2005;120 (5):649–661. [PubMed: 15766528]

Kim HJ, Chakravarti N, Oridate N, Choe C, Claret FX, Lotan R. N-(4 hydroxyphenyl)retinamide-induced apoptosis triggered by reactive oxygen species is mediated by activation of MAPKs in head and neck squamous carcinoma cells. Oncogene 2006a;25(19):2785–2794. [PubMed: 16407847]

Kim YM, Reed W, Wu W, Bromberg PA, Graves LM, Samet JM. Zn2+-induced IL 8 expression involves AP-1, JNK, and ERK activities in human airway epithelial cells. Am J Physiol Lung Cell Mol Physiol 2006b;290(5):L1028–1035. [PubMed: 16373669]

Knoch ME, Hartnett KA, Hara H, Kandler K, Aizenman E. Microglia induce neurotoxicity via intraneuronal Zn+2 release and a K+ current surge. Glia 2008;56:86–96.

Koh JY, Choi DW. Zinc toxicity on cultured cortical neurons: involvement of N-methyl-D-aspartate receptors. Neuroscience 1994;60(4):1049–1057. [PubMed: 7936205]

Koh JY, Suh SW, Gwag BJ, He YY, Hsu CY, Choi DW. The role of zinc in selective neuronal death after transient global cerebral ischemia. Science 1996;272(5264):1013–1016. [PubMed: 8638123]

Land PW, Aizenman E. Zinc accumulation after target loss: an early event in retrograde degeneration of thalamic neurons. Eur J Neurosci 2005;21(3):647–657. [PubMed: 15733083]

Levinthal DJ, DeFranco DB. Reversible oxidation of ERK-directed protein phosphatases drives oxidative toxicity in neurons. J Biol Chem 2005;280(7):5875–5883. [PubMed: 15579467]

Li Y, Maher P, Schubert D. A role for 12-lipoxygenase in nerve cell death caused by glutathione depletion. Neuron 1997;19(2):453–463. [PubMed: 9292733]

Luo Y, DeFranco DB. Opposing roles for ERK1/2 in neuronal oxidative toxicity: distinct mechanisms of ERK1/2 action at early versus late phases of oxidative stress. J Biol Chem 2006;281(24):16436–16442. [PubMed: 16621802]

Maret W, Jacob C, Vallee BL, Fischer EH. Inhibitory sites in enzymes: zinc removal and reactivation by thionein. Proc Natl Acad Sci U S A 1999;96(5):1936–1940. [PubMed: 10051573]

McCulloch J, Dewar D. A radical approach to stroke therapy. Proc Natl Acad Sci U SA 2001;98(20): 10989–10991.

Meng TC, Fukada T, Tonks NK. Reversible oxidation and inactivation of protein tyrosine phosphatases in vivo. Mol Cell 2002;9(2):387–399. [PubMed: 11864611]

Murphy TH, Schnaar RL, Coyle JT. Immature cortical neurons are uniquely sensitive to glutamate toxicity by inhibition of cystine uptake. Faseb J 1990;4(6):1624–1633. [PubMed: 2180770]

Pal S, He K, Aizenman E. Nitrosative stress and potassium channel-mediated neuronal apoptosis: is zinc the link? Pflugers Arch 2004;448(3):296–303. [PubMed: 15024658]

Ryu H, Lee J, Zaman K, Kubilis J, Ferrante RJ, Ross BD, Neve R, Ratan RR. Sp1 and Sp3 are oxidative stress-inducible, antideath transcription factors in cortical neurons. J Neurosci 2003;23(9):3597–3606. [PubMed: 12736330]

Satoh T, Nakatsuka D, Watanabe Y, Nagata I, Kikuchi H, Namura S. Neuroprotection by MAPK/ERK kinase inhibition with U0126 against oxidative stress in a mouse neuronal cell line and rat primary cultured cortical neurons. Neurosci Lett 2000;288(2):163–166. [PubMed: 10876086]

Sensi SL, Jeng JM. REthiniing the excitotoxic milieu: the emerging role of Zn (2+) in ischemic neuronal injury. Curr Mol Med 2004;4(2):87–111. [PubMed: 15032707]

Seo SR, Chong SA, Lee SI, Sung JY, Ahn YS, Chung KC, Seo JT. Zn2+-induced ERK activation mediated by reactive oxygen species causes cell death in differentiated PC12 cells. J Neurochem 2001;78(3):600–610. [PubMed: 11483663]

Stanciu M, DeFranco DB. Prolonged nuclear retention of activated extracellular signal-regulated protein kinase promotes cell death generated by oxidative toxicity or proteasome inhibition in a neuronal cell line. J Biol Chem 2002;277(6):4010–4017. [PubMed: 11726647]

Tan S, Schubert D, Maher P. Oxytosis: A novel form of programmed cell death. Curr Top Med Chem 2001;1(6):497–506. [PubMed: 11895126]

Thomas GM, Huganir RL. MAPK cascade signalling and synaptic plasticity. Nat Rev Neurosci 2004;5 (3):173–183. [PubMed: 14976517]

Tonks NK. PTP1B: from the sidelines to the front lines! FEBS Lett 2003;546(1):140–148. [PubMed: 12829250]

Xia Z, Dickens M, Raingeaud J, Davis RJ, Greenberg ME. Opposing effects of ERK and JNK-p38 MAP kinases on apoptosis. Science 1995;270(5240):1326–1331. [PubMed: 7481820]

Yu JS. Activation of protein phosphatase 2A by the Fe2+/ascorbate system. J Biochem (Tokyo) 1998;124 (1):225–230. [PubMed: 9644267]

Zaman K, Ryu H, Hall D, O'Donovan K, Lin KI, Miller MP, Marquis JC, Baraban JM, Semenza GL, Ratan RR. Protection from oxidative stress-induced apoptosis in cortical neuronal cultures by iron chelators is associated with enhanced DNA binding of hypoxia-inducible factor 1 and ATF-1/CREB and increased expression of glycolytic enzymes, p21(waf1/cip1), and erythropoietin. J Neurosci 1999;19(22):9821–9830. [PubMed: 10559391]

Zhang Y, Wang H, Li J, Jimenez DA, Levitan ES, Aizenman E, Rosenberg PA. Peroxynitrite-induced neuronal apoptosis is mediated by intracellular zinc release and 12 lipoxygenase activation. J Neurosci 2004;24(47):10616–10627. [PubMed: 15564577]

Zhuo S, Dixon JE. Effects of sulfhydryl regents on the activity of lambda Ser/Thr phosphoprotein phosphatase and inhibition of the enzyme by zinc ion. Protein Eng 1997;10(12):1445–1452. [PubMed: 9543006]

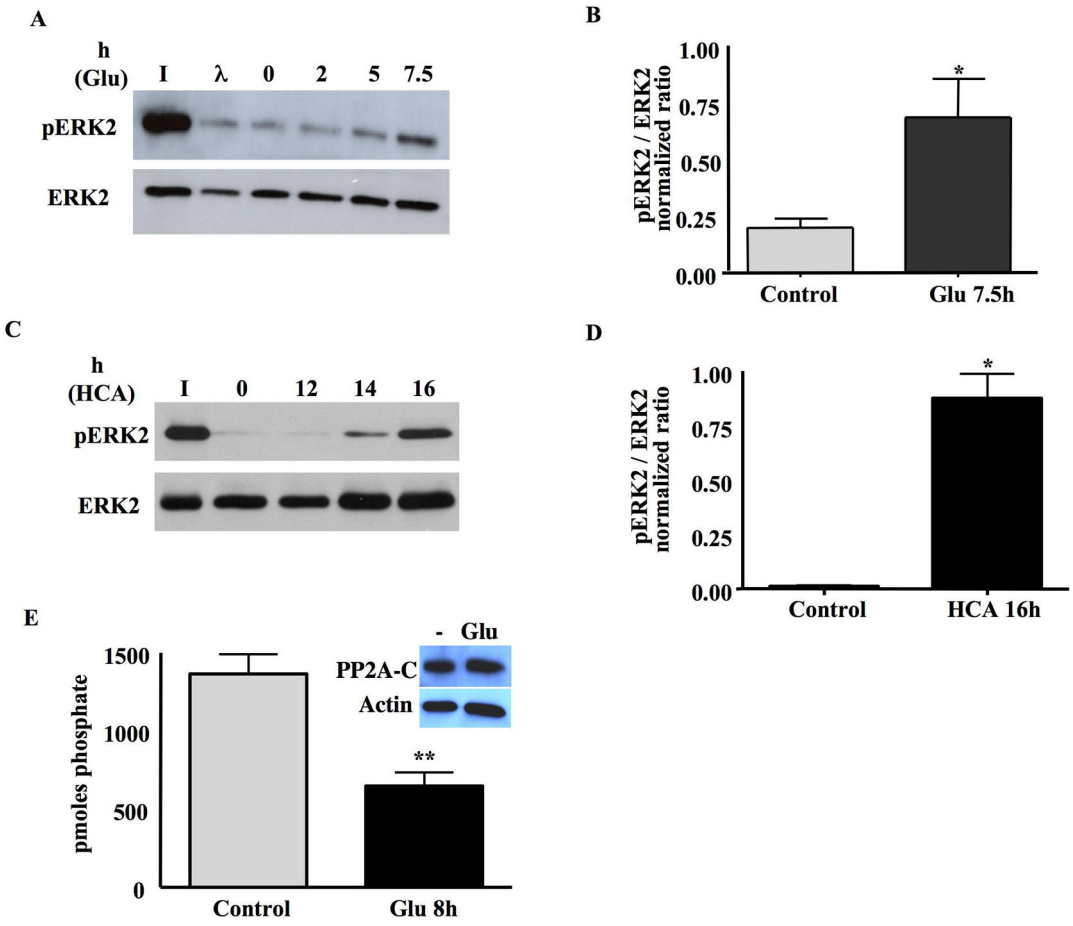

Fig 1. ERK2 phosphatase activity is inhibited upon oxidative stress in HT22 cells and immature neurons

A. HT22 cells were treated with 5mM glutamate for 0, 2, 5, or 7.5h. Whole cell lysates were incubated with purified, phosphorylated ERK2 (pERK2) and phosphatase activity was assessed by Western blots that revealed pERK2 or total ERK2. I=phosphatase assay input; λ=lambda phage protein phosphatase (positive control).

B. Quantification of the results from 4 independent experiments, revealing a significant decrease in ERK2 phosphatase activity following glutamate-induced oxidative stress in HT22 cells (mean±S.E.M, n=4). *$p<0.05$.

C. ERK2 phosphatase activity is inhibited upon 5mM HCA treatment immature neurons. Immature neurons were treated with HCA for 0, 12, 14, 16h. Whole cell lysates were incubated with purified pERK2 and phosphatase activity was assessed by Western blots that revealed either pERK2 or total ERK2. I=phosphatase assay input.

D. Quantification of the results from 3 independent experiments, revealing a significant decrease in ERK2 phosphatase activity following HCA-induced oxidative stress in immature neurons (mean±S.E.M, n=3). *$p<0.05$.

E. PP2A phosphatase activity in immunoprecipitates from HT22 cell extracts. PP2A was recovered by immunoprecipitation from whole cell lysates prepared from either untreated or 5 mM glutamate treated (8h) HT22 cells and phosphatase activity assayed using a synthetic phosphopeptide substrate. Activity normalized to PP2A C subunit recovered in immunoprecipitates is expressed as pmoles phosphate removed (mean±S.E.M, n=3, **$p<0.01$). Inset shows representative Western blot analysis of PP2A C subunit and β-actin expression in glutamate treated (8h) HT22 cells.

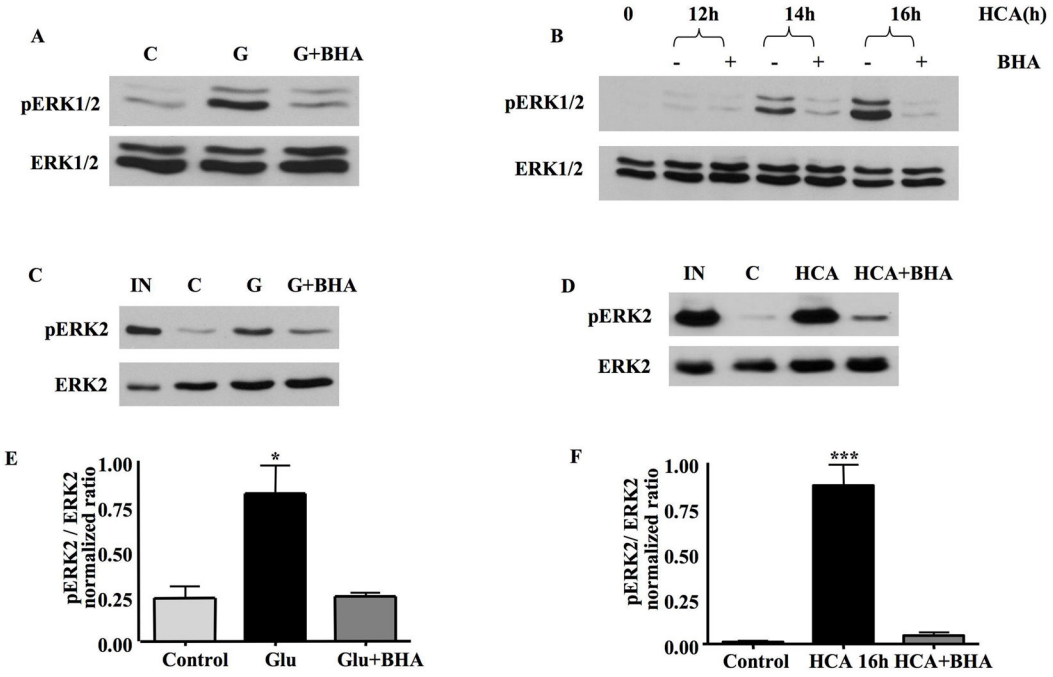

Fig 2. BHA blocks ERK1/2 activation and the inhibition of ERK2 phosphatase activity induced by oxidative stress in HT22 cells and immature neurons

A. HT22 cells were treated with glutamate or glutamate plus 100 μM BHA for 7.5h. 20μg of total protein lysate was separated by SDS-PAGE and subjected to Western blot analysis to detect pERK1/2 and total ERK1/2 on the same blots. C=control cell lysates. The addition of BHA blocked ERK1/2 activation following glutamate-induced oxidative stress.

B. Immature neurons were treated with HCA for 0, 12, 14 or 16 h in the presence or absence of BHA. 20μg of total protein lysate was separated by SDS-PAGE and subjected to Western blot analysis to detect pERK1/2 and total ERK1/2 on the same blots. The administration of BHA significantly blocks ERK1/2 activation following HCA treatment.

C. Whole cell lysates prepared from control untreated (C), glutamate (G)-treated or glutamate plus BHA treated HT22 cells were incubated with purified pERK2 and phosphatase activity assessed by Western blot that revealed either pERK2 or total ERK2. IN=ERK2 input. The addition of BHA reverses the glutamate-induced inhibition of ERK2 phosphatase activity.

D. Whole cell extracts prepared from the control (C), HCA-treated and HCA plus BHA treated immature neurons were incubated with purified pERK2 and phosphatase activity assessed by Western blot that revealed either pERK2 or total ERK2. IN=ERK2 input. The administration BHA reverses the inhibition of ERK2 phosphatase activity following HCA-induced oxidative toxicity.

E. Quantification of the results from 3 independent experiments. Co-administration of BHA abrogates the inhibition of ERK2 phosphatase activity in glutamate-treated HT22 cells (mean ±S.E.M, n=3). *$p<0.05$.

F. Quantification of the results from 3 independent experiments. Co-administration of BHA abrogates the inhibition of ERK2 phosphatase activity in HCA-treated immature neurons (mean±S.E.M, n=3). ***$p<0.001$.

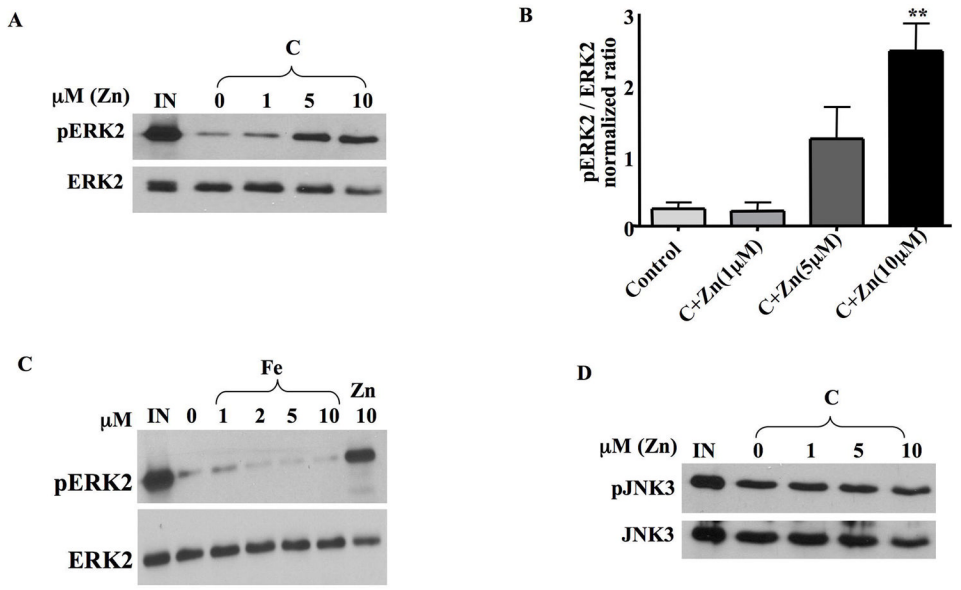

Fig 3. Zn^{2+} specifically inhibits ERK2 phosphatase activity in neuronal cell extracts

A. Various concentrations of $ZnCl_2$ were pre-incubated with whole cell lysates prepared from untreated HT22 cells for 10 min at 37ºC before the addition of pERK2 substrate. ERK2 dephosphorylation was monitored by Western blot analysis as described previously.

B. Quantification of the results from 3 independent experiments. 10μM $ZnCl_2$ significantly inhibits ERK2 phosphatase activity in HT22 cells (mean±S.E.M, n=3). **p<0.01.

C. Various concentrations of $FeCl_2$, and 10 μM $ZnCl_2$ as a control, were pre-incubated with whole cell lysates prepared from untreated HT22 cells for 10 min at 37ºC before the addition of pERK2 substrate. ERK2 dephosphorylation was monitored by Western blot analysis as described previously.

D. Various concentrations of $ZnCl_2$ were pre-incubated with whole cell lysates prepared from untreated HT22 cells for 10 min at 37ºC before the addition of pJNK3 substrate. JNK3 dephosphorylation was monitored by Western blot analysis as described previously. $ZnCl_2$ does not inhibit JNK3 phosphatase activity in HT22 cell extracts.

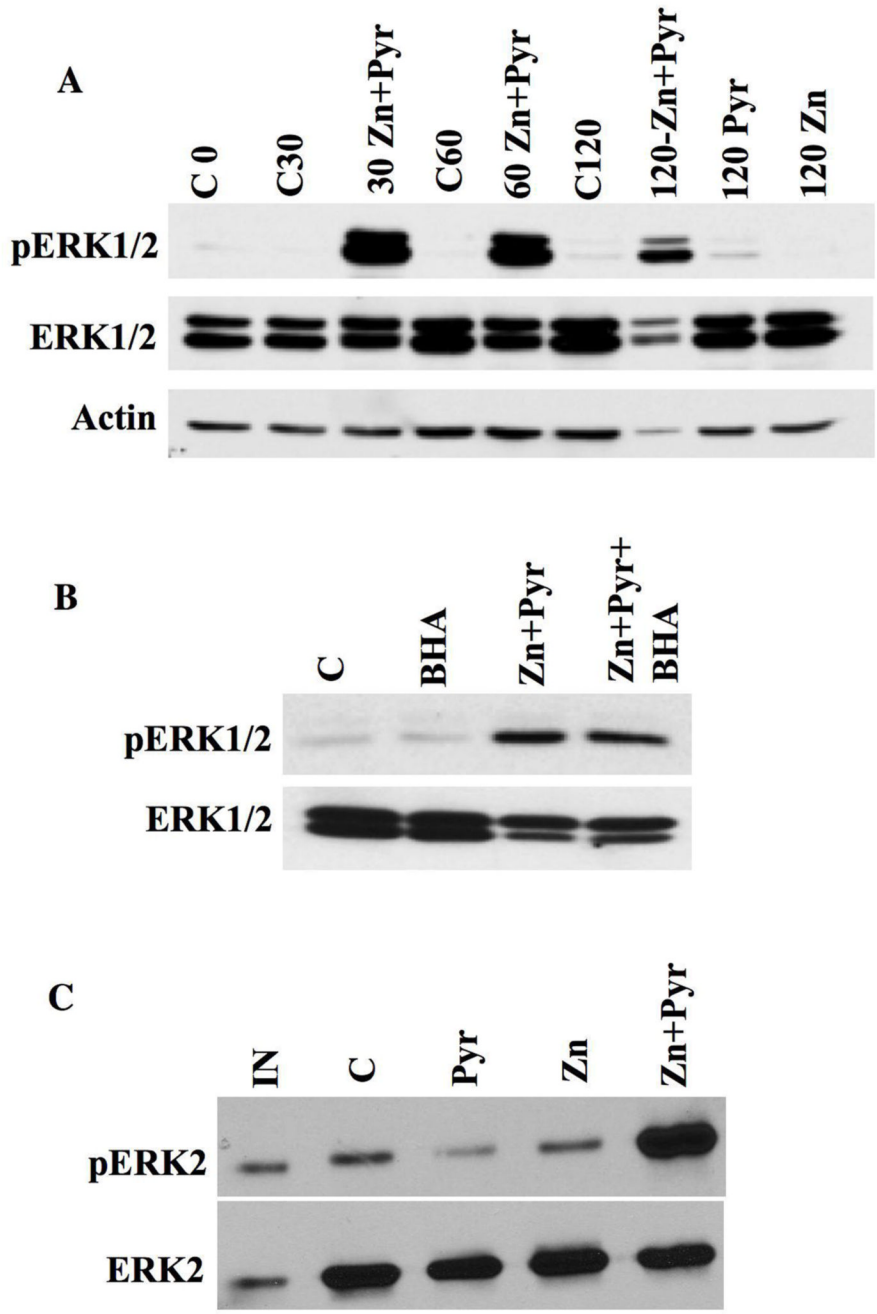

Fig 4. Zn^{2+} triggers ERK1/2 activation through direct inhibition of ERK1/2 phosphatases in the absence of oxidative stress

A. HT22 cells were treated with 10 μM $ZnCl_2$ (Zn), 5 μM sodium pyrithione (Pyr), or both compounds in serum-free medium for indicated times (30, 60, 120 min) followed by a 30 min recovery in serum-containing medium prior to harvesting. Control (C) conditions were performed without any additions but with a change from serum-free to serum containing medium that occurred at time 0. 20mg of total protein lysate was separated by SDS-PAGE and subjected to Western blot analysis to detect pERK1/2, total ERK1/2 and actin on the same blots. Blot shown is representative of three separate experiments where differences between

control conditions at each time point and combined $ZnCl_2$ and sodium pyrithione treatment groups were statistically significant ($p<0.015$).

B. HT22 cells were treated for 30 min with either 100 mM BHA alone, $ZnCl_2$ and sodium pyrithione, or BHA plus $ZnCl_2$ and sodium pyrithione as described above with a 30 min recovery in serum-containing medium. Blot shown is representative of three separate experiments where differences between control and combined $ZnCl_2$ and sodium pyrithione treatment groups as well as $ZnCl_2$, sodium pyrithione and BHA groups were statistically significant ($p<0.01$).

C. Whole cell lysates prepared from control untreated (C) or HT22 cells treated with 10 μM $ZnCl_2$ (Zn), 5 μM sodium pyrithione (Pyr), or both compounds (i.e. 30 min followed by 30 min recovery) were incubated with purified pERK2 and phosphatase activity assessed by Western blots that revealed either pERK2 or total ERK2. IN=pERK2 input. ERK2 phosphatase activity is inhibited by exposure of HT22 cells to $ZnCl_2$ and pyrithione. Blot shown is representative of three separate experiments where differences between control and combined $ZnCl_2$ and sodium pyrithione treatment groups were statistically significant ($p<0.05$).

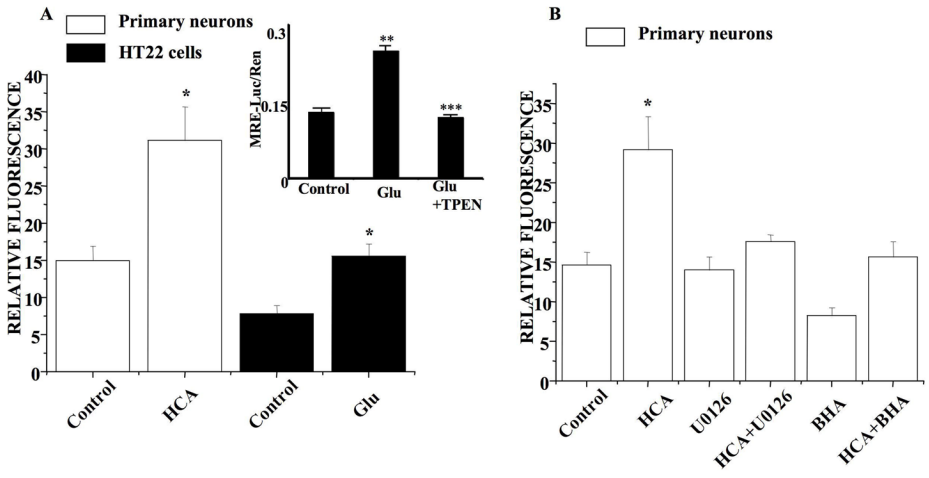

Fig 5. Oxidative stress triggers zinc accumulation in HT22 cells and immature neurons

A. HT22 cells were treated with glutamate for 8 h and immature neurons were treated with HCA for 12 h and loaded with FluoZin-3 for 30 min. The fluorescence imaging of intracellular zinc was then monitored by digital fluorescence microscopy and relative fluorescence measured. There is a significant increase in zinc accumulation following oxidative stress in both HT22 cells (mean±S.E.M, n=8) and immature neurons (mean±S.E.M, n=6). Inset shows results of MRE-luciferase assay in HT22 cells that were either untreated (control), treated with 5 mM glutamate (Glu) or 5 mM glutamate plus 5 μM TPEN. Values shown are the means (± SEM) of three experiments each performed in quadruplicate with the firefly luciferase activity from the MRE –driven reported normalized to *Renilla* luciferase activity. Glutamate treatment leads to statistically significant (**p< 0.001) difference in relative MRE-driven luciferase activity from control untreated cultures, while TPEN addition blocked the glutamate-induced increase in MRE-driven luciferase activity (*** p< 0.001).

B. Immature neurons were treated with HCA, HCA+U0126, HCA+BHA as well as U0126 only and BHA only and then were loaded with FluoZin-3 to measure the relative fluorescence. Co-administration with 10 μM U0126 (in DMSO) decreases the zinc accumulation in HCA-treated immature neurons to basal levels (mean±S.E.M, n=6). Similarly, the co-administration of 100 μM BHA also decreases the zinc release in HCA-treated immature neurons (mean ±S.E.M, n=6).

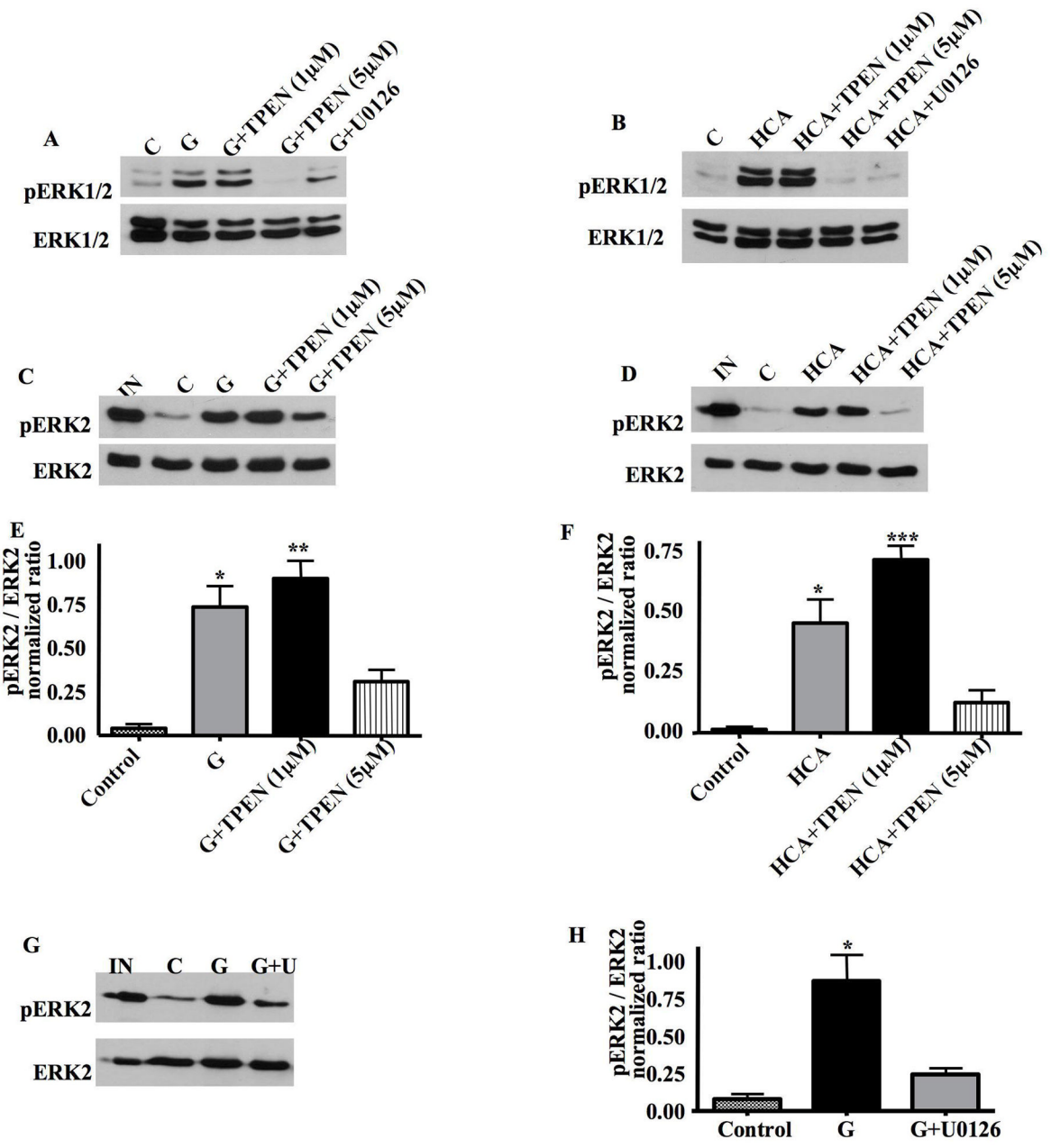

Fig 6. TPEN blocks ERK1/2 activation and reverses the inhibition of ERK2 phosphatase activity following oxidative stress in HT22 cells and immature neurons

A. HT22 cells were treated with glutamate, glutamate plus 1μM TPEN, glutamate plus 5μM TPEN, or glutamate plus U0126 for 8h. 20μg of total protein lysate was separated by SDS-PAGE and subjected to Western blot analysis to detect pERK1/2 and total ERK1/2 on the same blots. C=control cell lysates. 5μM TPEN blocks ERK1/2 activation following glutamate treatment in HT22 cells.

B. Immature neurons were treated with HCA, HCA plus 1μM TPEN, HCA plus 5μM TPEN, or HCA plus U0126 for 16h. 20μg of total protein lysate was separated by SDS-PAGE and subjected to Western blot analysis to detect pERK1/2 and total ERK1/2 on the same blots. C=control cell lysates. 5μM TPEN blocks ERK activation following HCA treatment in immature neurons.

C. An ERK2 phosphatase assay was performed on whole cell lysates prepared from untreated HT22 cells, or cells treated with glutamate, glutamate plus 1μM TPEN or glutamate plus 5μM TPEN. TPEN reverses the inhibition of ERK2 phosphatase activity following glutamate treatment in HT22 cells.

D. An ERK2 phosphatase assay was performed on whole cell lysates prepared from untreated immature neurons, or cells treated with HCA, HCA plus 1μM TPEN or HCA plus 5μM TPEN. TPEN reverses the inhibition of ERK2 phosphatase activity following HCA treatment in primary immature cortical neurons.

E. Quantification of the ERK2 phosphatase activity results from 3 independent experiments in HT22 cells (mean±S.E.M, n=3). There is significant difference between the group of glutamate-treated and glutamate plus 5μM TPEN (*$p<0.05$) as well as between the group of glutamate plus 1 μM TPEN and glutamate plus 5μM TPEN (**$p<0.01$).

F. Quantification of the ERK2 phosphatase assays results from 3 independent experiments in immature neurons (mean±S.E.M, n=3). There is significant difference between the group of HCA-treated and HCA plus 5μM TPEN (*$p<0.05$) as well as between the group of HCA plus 1 μM TPEN and HCA plus 5μM TPEN (***$p<0.001$).

G. An ERK2 phosphatase assay was performed on whole cell lysates prepared from untreated HT22 cells, or cells treated with glutamate, or glutamate plus 10μM U0126. The administration of U0126 reverses the inhibition of ERK2 phosphatase activity following glutamate treatment in HT22 cells.

H. Quantification of the ERK2 phosphatase assay results from 3 independent experiments in HT22 cells (mean±S.E.M, n=3). *$p<0.05$.

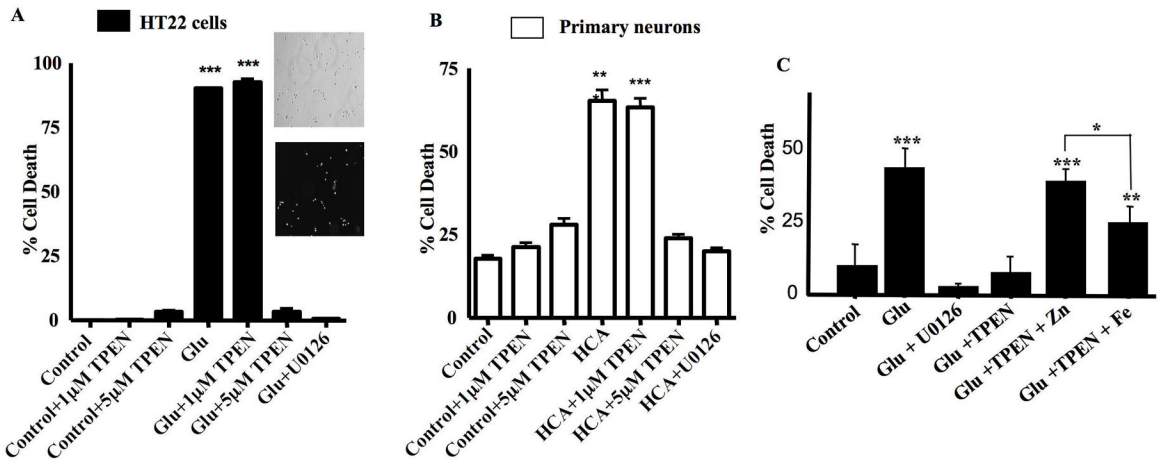

Fig 7. TPEN blocks oxidative toxicity in HT22 cells and immature neurons

A. HT22 cells were treated with 1μM TPEN, 5μM TPEN, 5 mM glutamate, glutamate plus 1μM TPEN, glutamate plus 5μM TPEN or glutamate plus 10μM U0126. Toxicity was measured as the percentage of PI-positive cells after treatment for 12 h (mean±S.E.M, n=3). ***p<0.001. 5μM TPEN blocks glutamate-induced oxidative toxicity in HT22 cells. Insets show typical results from a PI staining assay (with corresponding phase contrast images) from control untreated (Con) glutamate treated (Glu) cells.

B. Immature neurons were treated with 1μM TPEN, 5μM TPEN, 5mM HCA, HCA plus 1μM TPEN, HCA plus 5μM TPEN or HCA plus 10μM U0126. Toxicity was measured as the percentage of PI-positive cells after treatment for 16 h (mean±S.E.M, n=3).***p<0.001. 5μM TPEN blocks HCA-induced oxidative toxicity in immature neurons.

C. HT22 cells were treated with 5mM glutamate or glutamate with the following additions: 10μM U0126, 5μM TPEN, 5μM TPEN pre-incubated with 5μM $ZnCl_2$, and 5μM TPEN pre-incubated with 5μM $FeCl_2$. Toxicity was measured as the percentage of PI-positive cells after treatment for 12 h (mean±S.E.M, n=4). Toxicity was evaluated for statistical significance using One-way Analysis of Variance (ANOVA) with a Bonferroni Multiple Comparisons Test. ***p<0.001 and **p<0.01 relative to control. *p<0.05 when comparing toxicity between groups treated with glutamate and TPEN pre-incubated with $ZnCl_2$ versus those treated with glutamate and TPEN pre-incubated with $FeCl_2$.

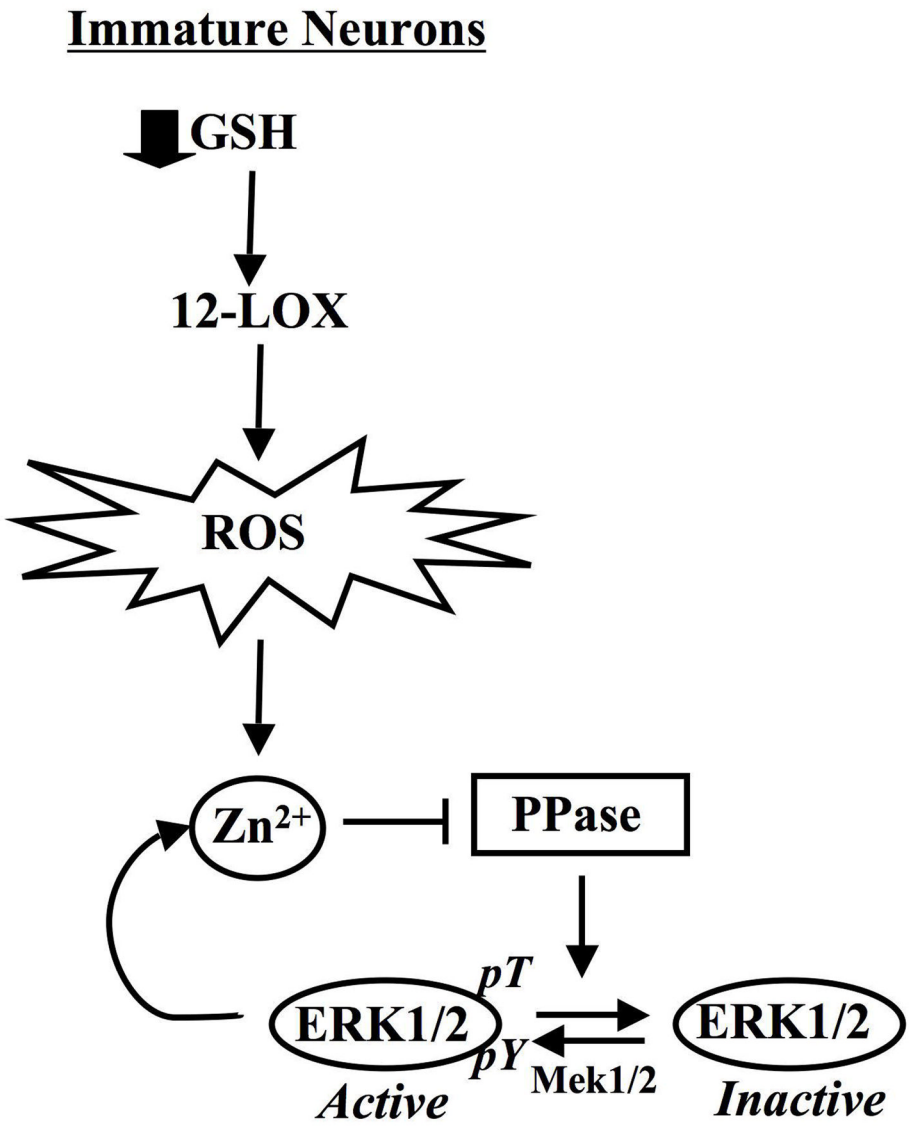

Fig 8. Mechanism of ERK1/2-dependent neuronal cell death triggered by ROS-mediated Zn^{2+} accumulation

Accumulation of intracellular Zn^{2+} brought about by oxidative stress (ROS) in neurons inhibits protein phosphatases that act selectively on ERK1/2. ROS are generated in immature neurons following the depletion of glutathione (GSH) and subsequent activation of 12-lipoxygenase (12-LOX). The persistent activation of ERK1/2 (pERK1/2) functions to promote cell death in part through a positive feedback loop that maintains elevated Zn^{2+} levels.